PB89-130454

Physical Factors Affecting Lung Deposition of Cigarette Smoke (with Syncarcinogenic Radon Progeny Effects), and Mineral Fiber Particulate Matter

Duke Univ. Medical Center, Durham, NC

Prepared for

Health Effects Research Lab.
Research Triangle Park, NC

Nov 88

U.S. Department of Commerce
National Technical Information Service
NTIS

TECHNICAL REPORT DATA
(Please read Instructions on the reverse before completing)

1. REPORT NO.	2.	3. RECIPIENT'S ACCESSION NO.
EPA/600/D-88/266		PB89 130454/AS

4. TITLE AND SUBTITLE
PHYSICAL FACTORS AFFECTING LUNG DEPOSITION OF CIGARETTE SMOKE (WITH SYNCARCINOGENIC RADON PROGENCY EFFECTS), AND MINERAL FIBER PARTICULATE MATTER.

5. REPORT DATE
November 1988

6. PERFORMING ORGANIZATION CODE

7. AUTHOR(S)
T. Martonen[1], W. Hofmann[2], I. Balásházy[3]

8. PERFORMING ORGANIZATION REPORT NO.

9. PERFORMING ORGANIZATION NAME AND ADDRESS
1= TB, ITD, HERL, U.S. EPA, RTP, NC 27711
2= Duke University, Durham, NC 27710
3= Central Institute of Physics, Budapest, Hungary

10. PROGRAM ELEMENT NO.

11. CONTRACT/GRANT NO.
68-02-4450

12. SPONSORING AGENCY NAME AND ADDRESS
Health Effects Research Laboratory, RTP
Office of Research and Development
U.S. Environmental Protection Agency
Research Triangle Park, NC 27711

13. TYPE OF REPORT AND PERIOD COVERED

14. SPONSORING AGENCY CODE
EPA-600/11

15. SUPPLEMENTARY NOTES

16. ABSTRACT

We address the unusual dynamic factors affecting the behavior and fate of inhaled cigarette-smoke particles and mineral fibers within the human lung. The actions of interception, for fiber particles, and cloud-settling, for concentrated cigarette smoke, can enhance focal deposition in locations that would not have been anticipated for dilute aerosols or for more regularly shaped, sphere-like particles. It is important to quantitate the efficiencies of these deposition mechanisms because it is after deposition that deleterious biological effects can occur. Here, we present theoretical deposition models that simulate the actions of the interception and cloud-settling processes, which are validated by comparisons with in vitro and in vivo data. The sites of preferential deposition are regions whose cells receive increased doses of hazardous substances associated with smokes and fibers. They must, therefore, be considered in risk assessment analyses of human inhalation exposures to airborne toxicants. Incorporation of these mechanisms in aerosol therapy protocols-the reverse of the usual inhalation toxicology concerns-could conceivable lead to improved therapeutic procedures, by which medications would be preferentially deposited at desired target locations within the lung so as to achieve optimal effects.

17. KEY WORDS AND DOCUMENT ANALYSIS

a. DESCRIPTORS	b. IDENTIFIERS/OPEN ENDED TERMS	c. COSATI Field/Group

18. DISTRIBUTION STATEMENT	19. SECURITY CLASS (This Report)	21. NO. OF PAGES
RELEASE TO PUBLIC	Unclassified	43
	20. SECURITY CLASS (This page)	22. PRICE
	Unclassified	A03/$3.95 / A06/$6.95

EPA Form 2220-1 (Rev. 4-77) PREVIOUS EDITION IS OBSOLETE

PB89-130454

EPA/600/D-88/266
November 1988

PHYSICAL FACTORS AFFECTING LUNG DEPOSITION OF CIGARETTE SMOKE (WITH SYNCARCINOGENIC RADON PROGENY EFFECTS), AND MINERAL FIBER PARTICULATE MATTER

Ted B. Martonen
Toxicology Branch
Inhalation Toxicology Division
Health Effects Research Laboratory
U.S. Environmental Protection Agency
Research Triangle Park, NC 27711

Werner Hofmann*
Center for Extrapolation Modeling
Duke University Medical Center
Durham, NC 27710

Imre Balásházy†
International Atomic Energy Agency
[Postdoctoral Fellowship]
U.S. Environmental Protection Agency
Research Triangle Park, NC 27711

*Permanent Address:
Abteilung fur Biophysik
Universität Salzburg
Hellbrunnerstr. 34
A-5020 Salzburg, Austria

†Permanent Address:
Central Research Institute for Physics
H-1525 Budapest, Hungary

EPA Contract 68-02-4450

EPA Project Officer
Ted B. Martonen

HEALTH EFFECTS RESEARCH LABORATORY
OFFICE OF RESEARCH AND DEVELOPMENT
U.S. ENVIRONMENTAL PROTECTION AGENCY
RESEARCH TRIANGLE PARK, NC 27711

REPRODUCED BY
U.S. DEPARTMENT OF COMMERCE
NATIONAL TECHNICAL INFORMATION SERVICE
SPRINGFIELD, VA. 22161

NOTICE

This document has been reviewed in accordance with U.S. Environmental Protection Agency policy and approved for publication. Mention of trade names or commercial products does not constitute endorsement or recommendation for use.

I. INTRODUCTION

In our contribution to this international symposium, we shall address dynamic factors affecting the behavior and fate of inhaled cigarette smoke particles and mineral fibers. We shall focus upon the rather unusual physical processes which influence their regional dispersion patterns within the human lung. The efficiencies of these deposition mechanisms are important to know as it is after deposition that deleterious biological effects can occur. As shall be demonstrated, the actions of 'interception' for fiber-shaped particles and 'cloud settling' for concentrated cigarette smokes can produce locations of enhanced deposition which would not have been anticipated, a priori, for dilute aerosols or more regularly shaped, sphere-like particles. These processes will result in the increased delivery of smoke and fiber particles to certain sites within the lung. These sites of highly localized deposition are regions of increased dosage, or exposure, of airway cells to hazardous substances associated with smokes and fibers and, therefore, must be dealt with in risk assessment analyses subsequent to a population's inhalation exposure to the airborne toxicants. [Note: it is interesting to contemplate that the incorporation of these mechanisms into aerosol therapy protocols--the opposite of inhalation toxicology concerns--could conceivably lead to improved regimens by which medicines are preferentially deposited at appropriate locations within the lung so as to elicit optimum therapeutic effects.]

II. BASIC PARTICLE MOTION AND INTERACTIONS

A. Single Particle Kinetics

For airborne particles that have relatively regular geometric forms (i.e., not linear, or fiber-like in dimensions) the deposition mechanisms of most efficiency are inertial, gravitational and diffusional in nature. These are illustrated in Figure 1. Inertial impaction (letter (A)) is effective when particles, carried by the airstream, have sufficient momentum to deviate from fluid streamlines and literally impact upon airway surfaces. Sedimentation (letter (B)) is most efficient in the lower, more peripheral, airways of the lung where airflow velocities have been sufficiently reduced--for a given inspiratory flow rate-- so that particle residence times in airways permit gravity to exert its effect. For submicron particles, the dominant selective maneuver of deposition is diffusion; see letter (C) in Figure 1. Other mechanisms of import, depending upon the substances of the inhaled aerosols and exposure conditions are electrophoretic, thermophoretic, etc. (Mercer, 1977) --and as we shall discuss, interception.

The motion of assemblages of particles and particulate media are subjects that have been treated extensively by Happel and Brenner (1973). Here, we shall address only those topics most salient to our intended evolution of a simulation of the phenomenon of cloud settling, to be described in due course.

The terminal settling velocity of an isolated solid spherical particle in a motionless fluid under viscous flow conditions may be expressed Stokes' Law (1845,1851) as

$$U_p = \frac{g\rho_p D_p^2}{18\mu} \qquad (1)$$

where ρ_p and D_p are the particle's material density and geometric diameter, respectively, g is the gravitational constant, and μ is the fluid's absolute viscosity. The conditions necessary for Equation (1) to be applicable to the size range of particles of concern in inhalation toxicology matters have been detailed by Fuchs (1964), and will not be repeated here for sake of brevity. The numerator of Equation (1) may, if deemed necessary, be modified by a slip correction factor as originally proposed by Cunningham (1910) in the form: $1 + 1.63\lambda/r_p$, where λ is the mean free path of air molecules and r_p the 'effective' radius of the particle under concern.

For a liquid droplet of viscosity μ' settling in the aforementioned fluid, Equation (1) now becomes

$$U_p = \frac{g\rho_p D_p^2}{18\mu} \quad \frac{3\mu' + 3\mu}{3\mu' + 2\mu} \qquad (2)$$

The velocity of the droplet is greater than that of a similarly sized solid particle because the resistive drag force acting upon it is lessened by the internal currents induced by tangential friction forces (see Figure 2). Equation (2) was derived independently by two investigators; Rybczynski (1911), and Hadamard (1911)--but since these works are difficult to access, we have cited their achievements via the manuscript of Smoluchowski (1912) in our REFERENCES.

B. Transitional Particle-Fluid Motion

The introduction of another particle, solid or droplet, in the vicinity of a first (as considered in preceding text) will have the effect of enhancing the rate of sedimentation, U_p', of both via mutual hydrodynamic interactions, see Figure 3, of the form

$$\frac{U_p'}{U_p} = 1 + \frac{3D_p}{8d}\left(1 + \cos^2\theta\right) + \left(\frac{D_p}{2d}\right)^2 \left(\frac{1}{3} - \cos^2\theta\right) \qquad (3)$$

where θ is angle between the line-of-centers between the particles and the vertical, and d is the distance between the centers. Other terms are as defined previously. The consideration of additional particles results in ever increasingly complex equations describing individual motion.

Whether particles are solid or liquid, their very presence alters the physical properties of the fluid entraining them. For example, Einstein in 1906 and 1911 [Note: These publications are listed in the Einstein (1956) book which we cite in our REFERENCE section; which we have done as it is in English, and we felt may be more available to our audience.] showed that the viscosity, μ_s, of a dilute, uniform suspension of spherical particles may be written in the form

$$\mu_s = \mu\left(1 + \frac{5}{2}\phi\right) \qquad (4)$$

where μ, as before, is the viscosity of the fluid <u>per se</u>, and ϕ is the volume fraction of particles present under consideration. This work, with others, is treated in the Happel and Brenner (1973) text, to which we refer the reader.

C. Aerosol Dynamics

The scientifid disciplines regarding particle kinetics and related fluid dynamics is rich in numerous and notable publications. Even a most cursory review of the subject is beyond the scope of this focused work. So, we refer the reader interested in the material to the works of Lamb (1932), Fuchs (1964) and Reist (1984, 1987), and text cited therein, for more information.

When the settling of an assemblage of particles within a 'bounded' medium such as air occupying the lung is investigated, it is important to distinguish

the case when particles are distributed throughout the fluid from the case when they are not. Although the settling particles create velocity fields which tend to increase the velocities of neighboring particles, mass conservation within the closed system requires that a fluid flow field exist in an opposite sense (to the particulate matter) to compensate for the settling particles and dragged fluid. If particles are dispersed then particle settling will be retarded because the compensating flow must penetrate, rather than bypass, the particle array. This may be termed hindered settling. If the particles are not dispersed, this compensating flow will occur mainly in particle-free regions and will not, effectively, retard particle settling. With the placement of an increasing number of particles in a specified region, the fluid experiences increasing resistance as it flows through the spatial arrangement of particles. As long as this penetration continues, individual particle settling, even as modified by mutual hydrodynamic interactions, can be thought to exist. Soon, however, the path of least resistance for the fluid will be to flow partially around the space occupied by the particles rather than to penetrate the array entirely (Fuchs, 1964). At this point, the particle array begins to develop the nature of an entity and attains a certain velocity as a whole which is superimposed upon the settling velocities of the individual particles relative to it. This effect will continue to increase with the addition of particles in the space. Finally, as the concentration is further increased, individual particle settling is finally completely masked as fluid no longer penetrates the array at all but rather flows around it. At this stage, cloud settling exists, and its motion may be considered to be that of a fluid sphere settling through a surrounding fluid of differing material properties (see Equations (2) and (4)); see Figure 4.

Smoluchowski (1911) expressed the settling velocity of a spherical cloud, U_c, in an 'unbounded'--for mathematical simplicity--medium as

$$U_c = \frac{2g\rho_c R_c^2}{9\mu} \frac{3\mu_c + 3\mu}{3\mu_c + 2\mu} \qquad (5)$$

where the new parameters are: μ_c is the viscosity of the cloud in the bracketed Rybezynski (1911) and Hadamard (1911) correction term (see Equation (2)); and, ρ_c and R_c are the density and geometric radius of the cloud, respectively. [Note: the concepts of 'bounded' versus 'unbounded' fluid dynamics problems are definite, important distinctions, from engineering perspectives. We add this, simply because many of our colleagues in attendance here at the symposium, as well as some readers, may not be from physical science disciplines]. He assumed that the cloud was dilute, so that the fractional solid volume, ϕ, was negligible and $\mu_c = \mu$ (see Equation (4)). And, that the cloud's density, or particulate mass concentration, (relative to the surrounding medium) could be written as

$$\rho_c = N_p \rho_p \left(\frac{r_p}{R_c}\right)^3 \qquad (6)$$

where N_p is the total number of particles in the cloud, and r_p its geometric radius, respectively. Equation (5) could then be rewritten as

$$U_c = \frac{4gN_p\rho_p r_p^3}{15\mu R_c} \qquad (7)$$

emphasizing the constituent particulate matter properties. Smoluchowski pointed out that Stokes' (1845, 1851) law is not an accurate description of particle motion unless cloud settling is <u>not</u> significant, a condition which we may formulate as $U_c << Up$, or, from Equations (1) and (7),

$$\frac{6N_p r_p}{5R_c} << 1 \quad . \tag{8}$$

At the time of his derivation, there was no experimental data to validate the theoretical findings.

Apparently unaware of Smoluchowski's (1912) theoretical work (i.e., it was not cited), Slack (1963a, 1963b) has conducted tests which we feel have demonstrated the existence of cloud settling experimentally, although he did not use such terminology. He examined the sedimentation under gravity of spherically shaped suspensions of spherical Diakon® particles in still air. The investigations revealed that 50 cm diameter monodisperse suspensions, which contained as little as 2 grams of particulate matter of geometric diameter < 64 μ distributed within, developed--and sustained--internal circulations. These currents were directed upward at the periphery of the suspensions and downward at their center; as illustrated in Figure 2 in this text for a liquid droplet. The existence of the circulatory flow patterns within the suspensions indicated, we surmise, that air was flowing around, rather than penetrating the arrays of settling particulate matter. For 10 μ particles settling in the experiments, with $\rho_p = 1.18$ gm cm^{-3}, the total number of particles in the suspensions may be shown to be approximately $N_p = 3 \times 10^7$ so that the condition of Equation (8) is easily satisfied. Smoluchowski's (1912) earlier theoretical model, now substantiated, thus predicted the interactive particle motion and cloud settling effects observed later by Slack (1963a, 1963b) in the laboratory.

To express the influence of particulate mass concentration, ρ_c, upon the transition from single particle motion-to hydrodynamic interactions-to the onset of cloud settling, Equation (8) may be put into the form

$$\frac{6}{5}\frac{\rho_c}{\rho_p}\left(\frac{R_c}{r_p}\right)^2 \ll 1 \quad . \tag{9}$$

In the aforementioned tests of Slack (1963a, 1963b) the value of ρ_c was 3.1×10^{-3} gm cm^{-3}, at cloud settling conditions.

D. Interception

There are, of course, a wide range of fibres of health effects concern--ranging from naturally occurring mineral fibers such as forms of asbestos to man-made glass fibers (Joint ACGIH-AIHA Aerosol Hazards Evaluation Committee, 1975; HEW Publication No. (NIOSH) 76-151, 1976; Spurny, 1983).

For airborne mineral fiber particles, a significant deposition mechanism is termed interception. The physical moves are shown in Figure 5, for three selected particle orientations--relative to fluid flow patterns. Interception is important when--even through a particle's center of mass remains on a fluid streamline--it can still come in contact with an airway wall. Of course, particle orientation is a most relevant factor to be considered in computing the deposition efficiency of mineral fibres. In Figure 5, we illustrate three specific instances of rod-shaped particle motion. In case (A), we assume the fiber to be arranged in a longitudinal fashion to entraining fluid motion. For case (B), we treat a particle in an assigned

spatial fix as to be perpendicular to a streamline transporting it. In (C) we consider a randomly moving fiber. Obviously, cases (A) and (B) may be thought to be 'boundary conditions', whereas, in reality, a tumbling fiber could be the more probable, realistic case.

Timbrell (1965) has experimentally demonstrated that there is no preferential orientation for fibers with an aspect ratio (i.e., a length-to-diameter ratio) of less than 5, while rod-like fibers tend to align themselves with the streamlines if their aspect ratio is larger than 5. In case of the latter orientation of inhaled fibers, the key deposition parameter of the interception mechanism is the fiber's diameter and not its length, and the penetration of fibers within the airway system is given by their aerodynamic equivalent diameter [Note: the aerodynamic equivalent diameter is defined as the diameter of a unit density sphere having the same terminal settling velocity (see Equation (1)) as the particle considered]. The aerodynamic equivalent diameter and the terminal settling velocity will obviously depend on the orientation of a fiber relative to the fluid within which it is moving.

Harris and Fraser (1976) have proposed mathematical expressions for the probability of the interception deposition mechanism of straight, cylindrical fibers at airway bifurcations and at the entrance of alveoli as functions of airway geometry and fiber characteristics for different airflow profiles and fiber orientations. Later, Harris and Timbrell (1977) extended this mathematical concept to incorporate irregularly-shaped or aggregated fibers. While Harris and Fraser (1976) assumed that all deposition mechanisms acting upon fibers are independent from each other, Harris and Timbrell (1977) considered the simultaneous action of impaction and interception. In a recent theoretical

effort we have developed a model for the simultaneous action of impaction, sedimentation, and interception deposition of fibers in a single bend tube of circular cross-section simulating an airway bifurcation (Balásházy et al., 1988).

Recently, Myojo (1987) measured the deposition of glass fibers in a single bifurcation (branching angle 45°) of a machined, brass model which corresponded approximately to the junction between generations 3 and 4 of Weibel's (1963) Model A. In Myojo's tests considered here, the length of the fibers was 20 - 40 μ, with an average diameter of 0.52 μ. Although the density of the fibers was not reported in the cited manuscript, we derived a value of 1.28 g/cm^3 from the published aerodynamic equivalent diameter for random orientation of the fibers within the bifurcation. In our mathematical simulations of these experimental data we assumed that interception occurs only within a distance $D_d/4$ of the 'daughter' airway, with diameter D_d, from the airflow dividing point, or carinal ridge.

In Figure 6 our model predictions are compared to Myojo's (1987) experimental results, presenting the deposition velocity as a function of the distance from the carina along the inner part of a 'daughter' airway. It can be seen that the measured deposition velocity lies between the calculated values for the deposition of fibers moving parallel to the streamlines (see (A) of Figure 5) and those for randomly oriented fibers (see (C) of Figure 5). This finding is supported by the experimental results of Timbrell (1965) for symmetric fibrous particles, and by the scanning electron microscope pictures shown by Myojo (1987). It is important to note that the maximum of the deposition velocity occurs directly at the carinal ridge, suggesting that potential health effects of inhaled fibers are caused preferentially at bifurcation sites.

III. CIGARETTE SMOKE DEPOSITION

Since the heterodisperse manner in which inhaled particulate matter is distributed within lung airways is of import to our text, we must now define a few simple morphological terms for subsequent applications. And, refer to some cigarette smoke particle-size parameters for deposition considerations.

Following Weibel's (1963) symmetric, dichotomously dividing Model A, we shall consider an airway branching site to consist of a 'parent' dividing into two 'daughters'. The 'daughters' will consist of two tubular segments with a common bifurcation zone; see Figure 7. The carinal ridge is the airstream divider at the junction of the 'daughter' airways, within the bifurcation zone.

Regarding particle size, the works of Sam (1956) and Keith and Derrick (1960) suggest that cigarette smokes have aerodynamic diameters in the 0.1 - 1.0 μ range, with the prevalent (based on a number frequency) being $\cong$ 0.2 - 0.25 μ. It is salient to comment that aerosols of such size may be anticipated to penetrate the upper (the oro- and nasopharyngeal, laryngeal and large-sized, upper bronchial airway regions) of the human respiratory tract to, and be deposited in, the more peripheral airways of the tracheobronchial tree and distal pulmonary passages (Task Group on Lung Dynamics, 1966; Lippmann, 1969; Heyder *et al.*, 1986).

A. *In Vitro* Experiments

Ermala and Holsti (1955) studied the deposition of tobacco smokes within full-scale plaster models of the human respiratory tract. Locations of

enhanced deposition were detected in the mouth-throat, larynx, and at airway branching areas (the bifurcation zone of Figure 7) in large bronchi of the simulator.

Complementary studies using Silastic® silicone rubber surrogate of human oropharyngeal-laryngeal-upper tracheobronchial regions have been presented by Martonen and Hofmann (1986) and Martonen et al. (1987). The findings confirmed the earlier data, and revealed two additional sites of preferential deposition for cigarette smokes: (1) highly localized deposits of deposited particulate matter were noticed at carinal ridges within upper bronchial bifurcation zones, and (2) along posterior surfaces of the tubular segments of 'daughter' airways (see Figure 7).

In the Ermala and Holsti (1956), and Martonen and Hofmann (1986) and Martonen et al. (1987) tests, the upper surrogate bronchial airways--where deposition was enhanced--correspond to in vivo main, lobar, segmental, subsegmental, and first generation of subsegmental bronchi. This may be related to a very interesting feature--namely, the predilection lung carcinomas have for certain locations, as noted in following text.

B. In Vivo Experiments

There is clinical evidence that carcinogenic tumors occur primarily in the main, lobar and segmental airways of the human lung (Bryson and Spencer, 1951; Herman and Crittenden, 1961; Garland, 1961; Garland et al., 1962). Additional findings are consistent with such cancers perhaps being originated within bifurcations (Kotin and Falk, 1959; Auerbach et al., 1961). It is, of course, not possible to establish with certainty the preferential morphological sites

of cancer, as most tumors are detected in advanced stages of development. [Note: Schlesinger and Lippmann (1978) referred to the 'striking correlation' between locations of clinically observed frequencies of distributions of tumors among the five lobar bronchi of the human lung, and aerosol patterns they measured within laryngeal-bronchial replica casts (see Figure 1 of that text)]. Although the deposition tests were not conducted with cigarette smokes, some experiments were done with particles in the 0.26 - 1.2 μ size range, similarly-sized to cigarette smokes as discussed in our preceeding text.

Hicks et al. (1986) have conducted inhalation exposure experiments with human test subject volunteers, attempting to ascertain the influences of hygroscopicity dynamics upon the deposition of aerosols. (The possible role of hygroscopic growth affecting the deposition of cigarette smoke within human lungs had been earlier noted by Davies (1974)). They studied the effect of the degree of aerosol growth for two aerosols: mainstream cigarette smoke and sodium chloride. The results of their laboratory investigations are plotted in Figure 8. The sizes of the aerosols were measured directly with a quartz crystal microbalance cascade impactor pre-inhalation and post-exhalation. The researchers deduced that the inhaled cigarette smoke particles had an increased growth factor of approximately 1.7, whereas sodium chloride aerosols were indicated to have grown by a factor of about 4.5. Nevertheless, the deposition--of comparatively sized inhaled particles--of the smoke aerosols was much greater.

Since cigarette smoke and sodium chloride particles did have much different growth factors, Hicks et al. (1986) expected the two aerosols to have distinctive deposition patterns. But, this was obviously not the case, as the

minimum of total deposition occurred at particle sizes of $\cong 0.15\ \mu$ for both. This suggested to the authors therefore, that: "...there are other mechanisms contributing to the deposition pattern of cigarette smoke." No explanations, however, were conceived or submitted.

C. Cloud Settling in the Lung and Surrogate Models

Based upon the cigarette smoke characterization works of Sam (1960), Keith and Derrick (1960) and Keith and Tesh (1966), Martonen (1977) (see also Stöber et al. 1978) has shown that the particulate number (for use in Equation (8)) and mass (for use in Equation (9)) concentrations of cigarette smoke are $N_p \cong 3 \times 10^{+9}$ particles cm^{-3} and $\rho_c \cong 10^{-4}$ gm cm^{-3}, respectively. Cigarette smoke has, therefore, the necessary physical parameters regarding sufficient constituent particles--in terms of number and/or mass--for the cloud settling effect to be manifested (refer to the Slack (1963a, 1963b) tests cited above for magnitudes of relevant, comparable physical parameters). So, in the interest of scientific speculation (which is the stated intention of this international symposium to promote in a responsible fashion), we feel that the incidence of cloud settling within the lungs of the human test subjects of Hicks et al. (1986) could partially explain their interesting findings. Especially so, since in this work, we are introducing a mathematical basis for cloud settling motion. Similarly, the enhanced deposition of cigarette smoke in respiratory tract simulators observed by Ermala and Holsti (1955), and Martonen and Hofmann (1986) and Martonen et al. (1987), are consistent with the proposed action of cloud settling.

Here, we surmise that the onset of cloud settling within a bounded medium --as within the lung and surrogate models--is dependent upon a physical

situation which permits fluid to flow around a spatial array of particles. This is possible when a free surface exists at an interface between a particle array and its entraining medium. The formation, size and shape of clouds will depend primarily upon the fluid dynamics and geometry of the problem considered. Once created, the magnitude of the cloud settling effect depends upon the constituent particle concentration. [Note: the existence of cylindrical clouds in aerosol spectrometers (instruments used to aerodynamically characterize airborne particles) has been demonstrated by Martonen (1977)].

The occurrence of flow separation, the instance when an airstream is disjoined from a bounding surface, has been experimentally observed by Schroter and Sudlow (1969) in idealized surrogate laboratory models and replica casts of bifurcations of the human lung; and, in other scientific investigations performed at the Physiological Flow Studies Unit of Cambridge University, as catalogued by Pedley et al. (1977). Their studies were conducted using a variety of airway geometries and flow patterns simulating physiological conditions. A mathematical basis for the possibility of flow separation taking place in vivo has been predicted by the theory of Lakin and Fox (1974), which analyzed the fluid dynamics situations at airway branching sites within the tracheobronchial network. We hypothesize that, within the lung, the onset of flow separation may initiate the phenomenon of cloud settling.

IV. SYNCARCINOGENIC EFFECTS: CIGARETTE SMOKE AND RADON PROGENY

For cigarette smokers, the etiology of lung cancer may be affected by synergistic-carcinogenic interactions following exposures to naturally

occurring ambient radon progeny. We speak of 'synergism' if the combined effect of two toxic agents is given by the product of the two individual responses.

A recent analysis of lung cancer mortality among a cohort of caucasian underground uranium miners in the Colorado plateau demonstrates the existence of synergistic mechanisms between concurrent exposure to cigarette smoke and radon progeny (Whittemore and McMillan, 1983). The relative risk factor, R, expressed as a multiplicative function, is given by the formula

$$R = (1 + 0.31 \times 10^{-2}\ \mathrm{WLM})\ (1 + 0.51 \times 10^{-3}\ \mathrm{Pk}) \qquad (10)$$

where a miner's total exposure to radon decay products, termed daughters, is given in units of working level months (WLM) and referenced to cigarettes in packages (Pk) accumulated from the start of exposure until 10 years before the subject's current age.

Cigarette smoke may, however, have a paradoxical effect on concurrent exposure to radon progeny. Experimental data on beagle dogs (Cross et al., 1982) indicate a possible protective role of cigarette smoke, which could be ascribed to a stimulatory effect upon the mucociliary clearance process [Note: although the opposite effect has been observed in heavy, long-term human smokers], or an increased mucus production providing a shield, thereby limiting exposure, of underlying sensitive cells. Such possible factors may slightly reduce the lung cancer risk from radiation kinetics alone, but seem unlikely to compensate for the synergistic mechanism of cigarette smoke.

Experiments with rodents have shown that the order--or sequence,--in which cigarette smoke and radon exposures are administered is important (Cross,

1984). It appears that the absorbed energy of deposited radon progeny is the initiating event, and that cigarette smoke has a highly promotional effect. This would allow for the earlier occurrence of lung cancer by stimulated proliferation of cells that have already been transformed by ionizing radiation and/or other carcinogens, including chemical substances.

Earlier histological studies have noted highly localized pre-neoplastic and neoplastic lesions at airway bifurcations following inhalation exposures to cigarette smoke and other environmental pollutants (Kotin and Falk, 1959; Auerbach et al., 1961). In a study of human lung tissue specimens from deceased smokers, highly concentrated deposits of ^{210}Po were found in bifurcation zone epithelium of large bronchial airways (Little et al., 1965). Those authors concluded that alpha-radiation emitted from ^{210}Po may be an important factor in the initiation of bronchial cancers in smokers. Martell (1983) attributed the high incidence of malignant transformations at airway bifurcations in cigarette smokers to the cumulative alpha radiation dose due to enhanced deposition of insoluble ^{210}Po-enriched particles produced in burning cigarettes, but also to ambient radon progeny inhaled between cigarettes or contained as a constituent in mainstream cigarette smoke per se.

The latter idea has been developed and presented in more detail by Martonen and Hofmann (1986), Martonen et al. (1987), and Hofmann and Martonen (1988). In addition to enhanced deposition at airway branching sites, mucociliary clearance may be significantly slowed down, or reduced in efficiency, at such sites. A reduced rate of mucociliary clearance at the first tracheobronchial bifurcation has been measured in certain laboratory test animals (Gore and Patrick, 1978; Svartengren et al., 1981), with marked accumulations

of deposited particles discerned at the carina. In man, it has been experimentally observed that the rate of mucociliary clearance is slower within bronchial bifurcations, more distally to the level of segmental and subsegmental bronchi (Macklin, 1956; Hilding, 1957).

Based on the above described deposition and clearance patterns at airway bifurcations, we have developed a dosimetry model, in which each airway generation is divided into 3 distinct compartments: (1) two tubular airway segments with normal clearance rates, (2) a bifurcation zone (excluding the contiguous carina) with reduced clearance efficiency, and (3) a carinal ridge with no clearance at all (Hofmann and Martonen, 1988). It is our contention that these calculations suggest that the combined effect of enhanced radionuclide deposition--and reduced clearance at bronchial bifurcations, relative to tubular airway segments--may lead to highly localized accumulations of radon progeny within bifurcation zones, and, subsequently, to concentrated radiation doses delivered to sensitive, progenitor cells located at such sites.

It is important, we believe, to note that both inhaled radon progeny and cigarette smoke exhibit qualitatively the same non-uniform dose patterns. Under the assumption that cigarette smoke acts mainly as a promoting agent, the effect of cigarette smoke on lung cancer induction by inhaled radon progeny in the three compartments of an airway generation (lobar bronchi) is illustrated in Table 1. Lung cancer risk for each exposure regimen is normalized to the integer 1, assuming: (1) that risk is proportional to the annual radiation dose for environmental radon progeny exposure and proportional to the local retention pattern for cigarette smoke inhalation, and (2)

that radiation and cigarette smoke interact in a synergistic, i.e., multiplicative fashion. These calculations clearly demonstrate that the predicted non-uniformity of radiation-induced lung cancer risk is aggravated by the interaction with cigarette smoke.

V. SUMMARY AND CONCLUSIONS

Cloud settling is a physical phenomenon in which a finite population of particles occupying a discrete region of space settles at a rate exceeding the Stokes (1845, 1851) terminal settling speed of a constituent particle of the cloud, even as modified by hydrodynamic interactions from surrounding particles. The presence of cloud settling, and the extent to which it influences individual particle trajectories, has been demonstrated by Martonen (1977) in aerosol particle sizing instruments; and, we feel, in the engineering-particle physics laboratory tests of Slack (1963a, 1963b). Moreover, we propose that the occurrence of cloud settling may explain the human test subject inhalation exposure data anomalies of Hicks *et al.* (1986) and the enhanced cigarette smoke deposits observed in surrogate lungs by Ermala and Holsti (1955), and Martonen and Hofmann (1986) and Martonen *et al.* (1987). The separation of flow at bifurcations within the bronchial tree, as has been observed experimentally *in vitro*, may permit the formation of aerosol clouds within the human lung. Such upper airway sites are established as having enhanced deposition *in vitro* and incidence of cancer *in vivo*; it seems reasonable to recommend, therefore, that further efforts be conducted to establish the significance of the cloud settling mechanism upon the distribution of inhaled particulate matter. Assuming that such formation does indeed occur, a simple analytical model has been developed here which predicts that cloud settling will take

place unless Equations (8) and (10) are valid. When applied to the case of cigarette smoke the theoretical model predicts that raw cigarette smoke may have to be significantly diluted before the influence of cloud settling upon the distribution of cigarette smoke particles within the lung can be completely neglected.

Because of the correlation between clinically observed bronchial carcinomas and enhanced deposition sites detected in the _in vitro_ tests, we propose that the tumors are elicited there because cigarette smokes are initially deposited at corresponding bronchial locations _in vivo_. Not, as is the most popular current school of thought, that the submicron-sized cigarette smoke particles are originally deposited in more distal regions of the lung and are subsequently transported to, and accumulated within (primarily due to reduced mucociliary clearance efficiency mechanisms) upper bronchial bifurcations.

Regarding simultaneous exposure to radon progeny and cigarette smoke, we surmise that interactions may increase the absolute number of lung cancer cases, see Equation (1), and affect the relative distribution within a given generation (refer to Table 1). Perhaps, considering the role of mucociliary clearance, the significance of cloud settling is more important for short-lived radionuclides, not chemical carcinogens. For example, for ^{210}Po, a naturally occurring component of cigarette smoke, or syncarcinogenic effects arising from interactions between cigarette smoke and ambient radon progeny exposures such as take place within household dwellings.

Exposure to mineral fibers may act in a manner similar to that discussed above for cigarette smoke. Thus, concurrent inhalation of fibers, in smokers

and non-smokers alike, may also increase synergistically the probability of lung cancer induction due to the naturally occurring radon progeny.

REFERENCES

Auerbach O.; Stout A.P.; Hammond E.C.; Garfinkel L. Changes in bronchial epithelium in relation to cigarette smoking and in relation to cancer. New Engl. J. Med. 265:253-267; 1961.

Balásházy I.; Hofmann W.; Martonen T.B. Fiber deposition in an airway bifurcation: simultaneous action of interception, impaction and sedimentation deposition mechanisms. Submitted to J. Aerosol Sci.; 1988.

Bryson C.C.; Spencer H. Carcinoma of the bronchus. Q.J. Med. 20:173-186; 1951.

Cross F.T.; Palmer R.F.; Filipy R.E.; Dagle E.G.; Stuart B.O. Carcinogenic effects of radon daughters, uranium ore dust and cigarette smoke in beagle dogs. Health Phys. 42:33-52; 1982.

Cross F.T. Radioactivity and cigarette smoke. Health Phys. 46:205-208; 1984.

Cunningham E. On the velocity of steady fall of spherical particles through fluid medium. Proc. Royal Soc. (London) 83:357-365; 1910.

Davies C.N. Deposition of inhaled particles in man. Chem. Indus. 1:441-444; 1974.

Einstein A. The theory of Brownian movement. New York: Dover; 1956.

Ermala P.; Holsti L.R. Distribution and absorption of tobacco tar in the organs of the respiratory tract. Cancer 8:673-678; 1955.

Fuchs N.A. The mechanics of aerosols. Oxford: Pergamon Press; 1964.

Garland L.H. Bronchial carcinoma. Lobar distribution of lesions in 250 cases. Calif. Med. 940:7-8; 1961.

Garland L.H.; Beier R.L.; Coulson W.; Heald J.H.; Stein R.L. The apparent sites of origin of carcinomas of the lung. Radiology 78:1-11; 1962.

Gore D.J.; Patrick G. The distribution and clearance of inhaled UO_2 particles on the first bifurcation and trachea of rats. Phys. Med. Biol. 23:730-737; 1978.

Happel J.; Brenner H. Low Reynolds number hydrodynamics. Leyden:Noordhoff International Publishing; 1973.

Harris, Jr. R.L.; Fraser D.A. A model for deposition of fibres in the human respiratory tract. Am. Ind. Hyg. Assoc. J. 37:73-89; 1976.

Harris, Jr. R.L.; Timbrell V. The influence of fibre shape in lung deposition - mathematical estimates. In: Inhaled Particles IV (Walton W.H., ed.) Oxford: Pergamon Press, pp. 75-89; 1977.

Herman D.L.; Crittenden M. Distribution of primary lung carcinomas in relation to time as determined by histochemical techniques. J. Natl. Cancer Inst. 27:1227-1271; 1961.

HEW Publication No. (NIOSH) 76-151. Occupational exposure to fibrous glass: proceedings of a symposium. Superintendent of Documents, U.S. Government Printing Office, Washington, D.C. 20402; 1976.

Heyder J.; Gebhart J.; Rudolf G.; Schiller C.F.; Stahlhofen W. Deposition of particles in the human respiratory tract in the size range 0.005-15 μm. J. Aerosol Sci. 17:811-825; 1986.

Hicks J.F.; Pritchard J.N.; Black A.; Megaw W.J. Experimental evaluation of aerosol growth in the human respiratory tract. In: Aerosols: Formation and Reactivity. Oxford: Pergamon Press, pp. 244-247; 1986.

Hilding A.C. Ciliary streaming in the bronchial tree and the time element in carcinogenesis. New Engl. J. Med. 256:634-640; 1957.

Hofmann W.; Martonen T.B. The significance of enhanced radionuclide deposition at bronchial bifurcations. Ann. Occup. Hyg. (in press).

Joint ACGIH-AIHA Aerosol Hazards Evaluation Committee. Background documentation on evaluation of occupational exposure to airborne asbestos. Amer. Ind. Hyg. Assoc. J. 36:91-103; 1975.

Keith C.H.; Derrick J.C. Measurement of the particle size distribution and concentration of cigarette smoke by the "Conifuge". J. Colloid Interface Sci. 15:340-356; 1960.

Keith C.H.; Tish P.G. Measurement of the total smoke issuing from a burning cigarette. Tobacco Sci. 61-64; 1966.

Kotin P; Falk H.L. The role and action of environmental agents in the pathogenesis of lung cancer. I. Air pollutants. Cancer 12:147-163; 1959.

Lakin M.B.; Fox V.G. Transient flow characteristics in an idealized bronchial bifurcation. Respir. Physiol. 21:101-117; 1974.

Lamb, Sir H. Hydrodynamics (Sixth Edition). New York: Dover Publications, Inc.; 1932.

Lippmann M.; Albert R.E. The effect of particle size on the regional deposition of inhaled aerosols in the human respiratory tract. Am. Ind. Hyg. Assoc. J. 30:257-275; 1969.

Little J.B.; Radford, Jr. E.P.; McCombs H.L.; Hunt V.R. Distribution of polonium 210 in pulmonary tissues of cigarette smokers. New Engl. J. Med. 273:1343-1351; 1965.

Macklin C.C. Induction of bronchial cancer by local massing of carcinogen in outdrifting mucus. J. Thorac. Surg. 31:238-244; 1956.

Martell E.A. Alpha-radiation dose at bronchial bifurcations of smokers from indoor exposure to radon progeny. Proc. Natl. Acad. Sci. 80:1285-1289; 1983.

Martonen T.B. Aerosol characterization in a spinning spiral duct centrifuge. Ph.D. Thesis, University of Rochester, Rochester, New York; 1977.

Martonen T; Hofmann W. Factors to be considered in a dosimetry model for risk assessment of inhaled particles. Radiat. Prot. Dosim. 15:225-232; 1986.

Martonen T.B.; Hofmann W.; Lowe J.R. Cigarette smoke and lung cancer. Health Phys. 52:213-217; 1987.

Pedley T.J.; Schroter R.C.; Sudlow M.F. Gas flow and mixing in the airways. In: Lung biology in health and disease. New York: Marcel Dekker, Inc. pp. 163-265; 1977.

Postendörfer J.; Schraub A. Concentration and mean particle size of the main and side stream of cigarette smoke. Staub-reinhalt. Luft. 32:33-36; 1972.

Reist P.C. Introduction to Aerosol Science. New York: Mcgraw-Hill Book Co.; 1984. [Russian edition--Moscow: Mir Publishers; 1987].

Sam A. A study of particle size distribution and dilution of cigarette smoke. Ph.D. Thesis, Duke University, Durham, North Carolina; 1956.

Schlesinger R.B.; Bohning D.E.; Chan T.L.; Lippmann M. Particle deposition in a hollow cast of the human tracheobronchial tree. J. Aerosol Sci. 8:429-445; 1977.

Schlesinger R.B.; Lippmann M. Selective particle deposition and bronchogenic carcinoma. Environ. Res. 15:424-431; 1978.

Schroter R.C.; Sudlow M.F. Flow patterns in models of human bronchial airways. Respir. Physiol. 7:341-355; 1969.

Slack G.W. Sedimentation of a large number of particles as a cluster in air. Nature 200:1306; 1963a.

Slack G.W. Sedimentation of compact clusters of uniform spheres. Nature 200:466-467; 1963b.

Smoluchowski M.S. On the practical applicability of Stokes' Law of resistance and modifications of it required in certain cases. 5th International Conference of Mathematics, Cambridge, 2:192-201; 1911.

Spurny K.R. Measurement and analysis of chemically changed mineral fibers after experiments in vitro and in vivo. Environ. Hlth. Perspec. 51:343-355; 1983.

Stöber W.; Martonen T.B.; Osborne, Jr. S. On the limitations of aerodynamical size separation of dense aerosols with the spiral duct centrifuge. In: Recent developments in aerosol science. New York: J. Wiley and Sons. pp. 263-278; 1978.

Stokes, Sir G.G. On the theories of the internal friction of fluids in motion, and of the equilibrium and motion of elastic solids. Camb. Trans. VIII:287; 1845.

Stokes, Sir G.G. On the effect of the internal friction of fluids on the motion of pendulum. Camb. Trans. IX:8; 1851.

Svartengren M.; Widtskiöld-Olsson, K.; Philipson K.; Camner P. Retention of particles on the first bifurcation and trachea of rabbits. Bull. Europ. Physiopath. Resp. 17:87-91; 1981.

Task Group on Lung Dynamics. Deposition and retention models for internal dosimetery of the human respiratory tract. Health Phys. 12:173-207; 1966.

Timbrell V. The inhalation of fibrous dusts. Ann. N.Y. Acad. Sci. 132:255-273; 1965.

Weibel E.R. Morphometry of the lung. West Berlin: Springer-Verlag; 1963.

Whittemore A.S.; McMillan A. Lung cancer mortality among U.S. uranium miners: a reappraisal. JNCI 71:489-499.

TABLE LEGENDS

Table 1. Localized (morphological) lung cancer induction as related to inhalation exposure and aerosol composition.

FIGURE LEGENDS

Figure 1. Primary deposition processes for regularly-shaped particles in respiratory tract passages. The mechanisms are: (A) inertial impaction; (B) sedimentation; and, (C) Brownian motion.

Figure 2. Illustration of circulating currents within a liquid droplet caused by external drag forces.

Figure 3. A diagram of mutual hydrodynamic interactions between two moving particles.

Figure 4. The cloud settling phenomenon; when aerosols are of sufficient concentration to exhibit aerodynamic properties relatively independent of component particles.

Figure 5. The deposition of fiber-shaped particles at a branching division within lung airways.

Figure 6. A comparison of theoretically predicted and experimentally measured (plot 1) fiber deposition within a surrogate bifurcation. Computations are for fiber orientations, relative to fluid streamlines (see Figure 5), of: longitudinal, or parallel (plot 2), random (plot 3) and perpendicular (plot 4), alignment.

Figure 7. A description of a branching region between airways of succeeding generations.

Figure 8. A comparison of hygroscopic aerosol deposition in human subjects: 0 = cigarette smoke inhalation exposures, and Δ = sodium chloride.

TABLE 1

EXPOSURE PROTOCOL	LUNG CANCER RISK (%)		
	Tubular Airway Segments	Bifurcation Zone	Carinal Ridge
Rn progeny	7.34	18.80	73.85
Cigarette Smoke	0.56	8.69	90.76
Rn progeny and cigarette smoke	0.06	2.38	97.56

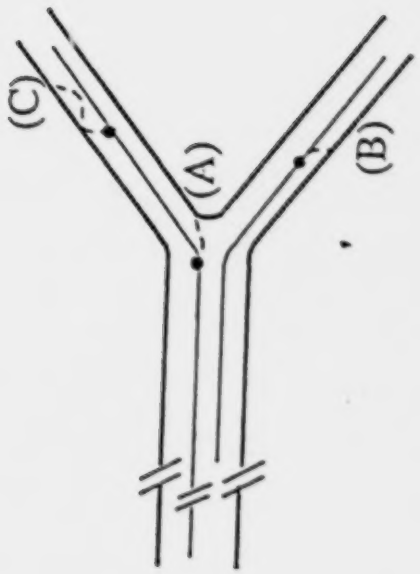

FIGURE 1

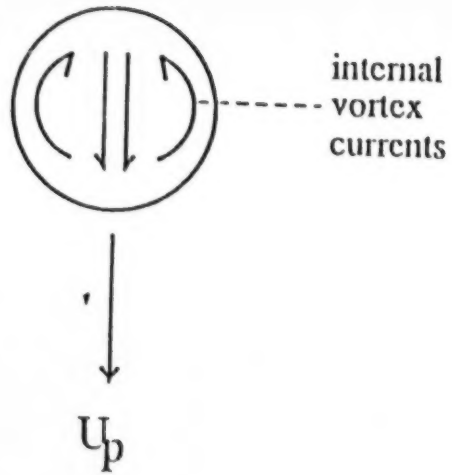

FIGURE 2

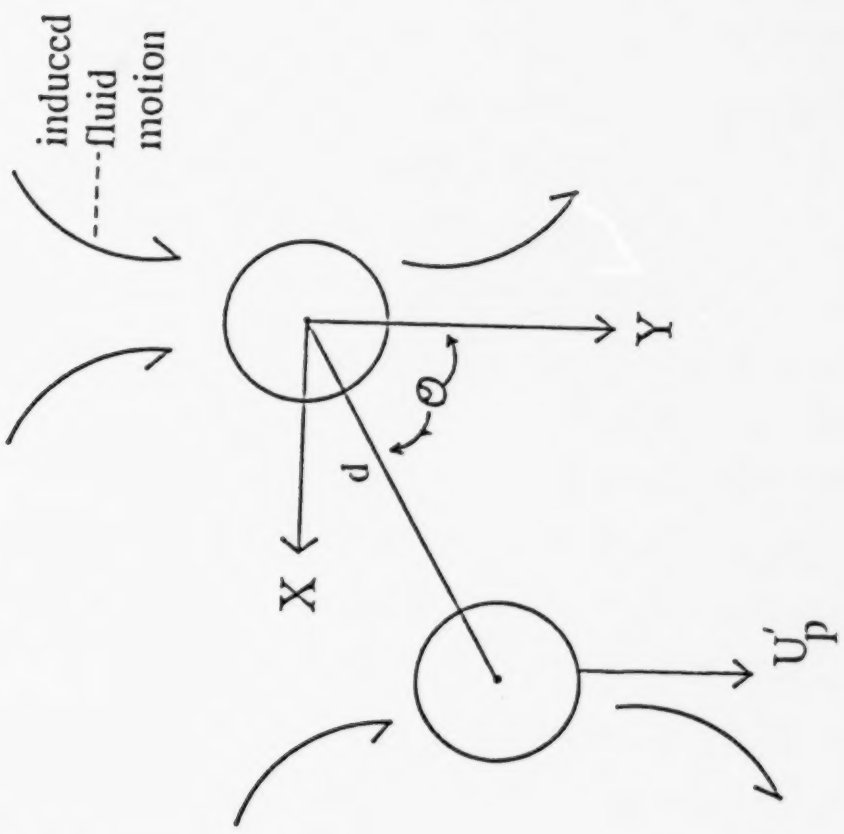

FIGURE 3

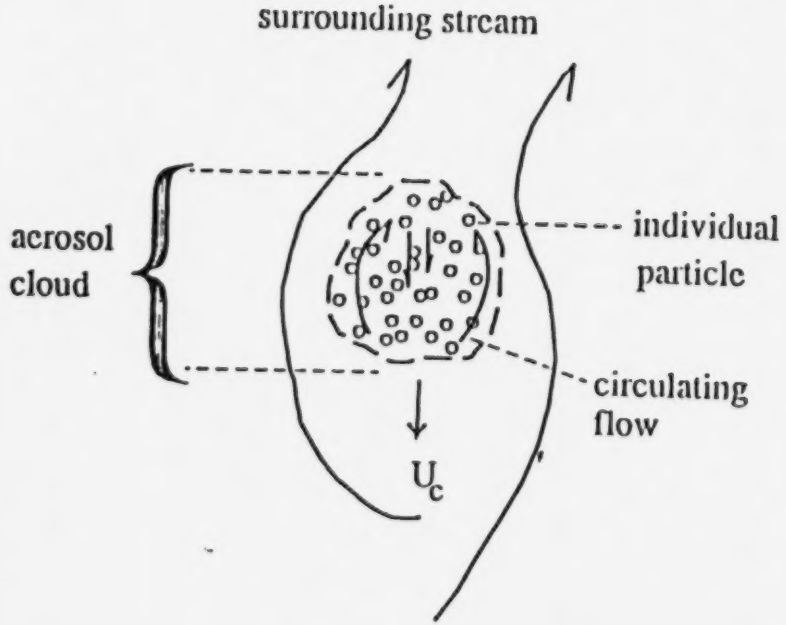
surrounding stream
aerosol
cloud
individual
particle
circulating
flow
U_c

FIGURE 4

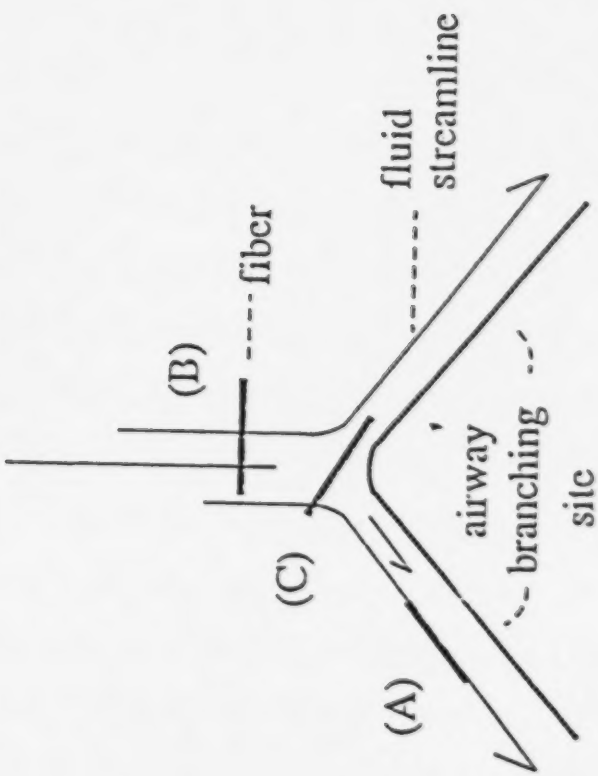

FIGURE 5

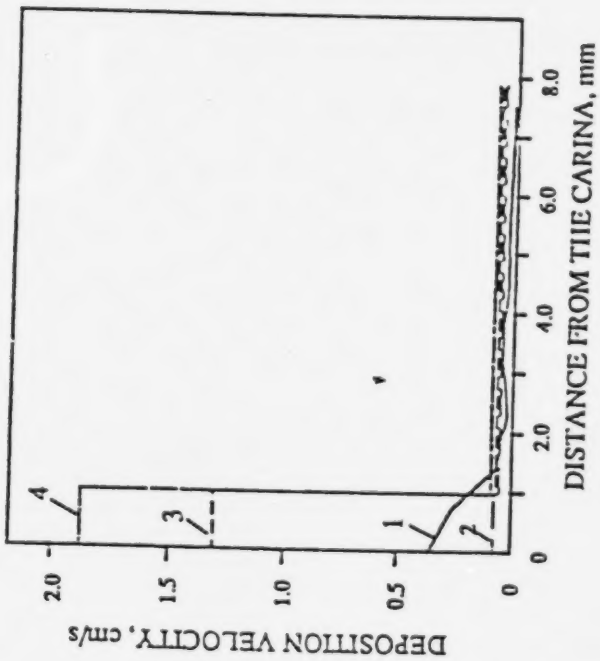
DEPOSITION VELOCITY, cm/s
2.0
1.5
1.0
0.5
0
4
3
1
2
0
2.0
4.0
6.0
8.0
DISTANCE FROM THE CARINA, mm

FIGURE 6

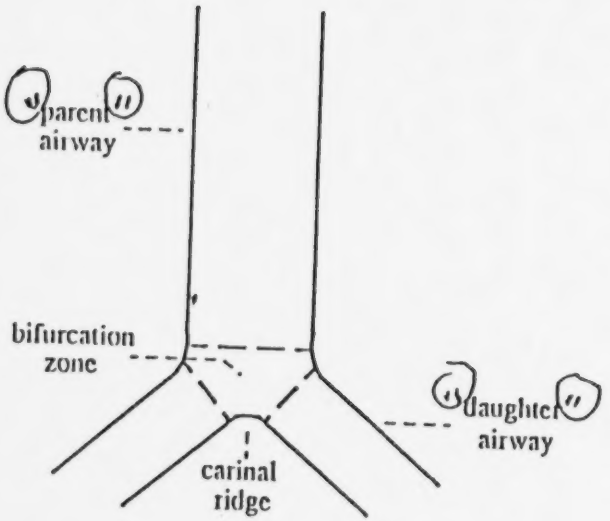
parent
airway
bifurcation
zone
daughter
airway
carinal
ridge

FIGURE 7

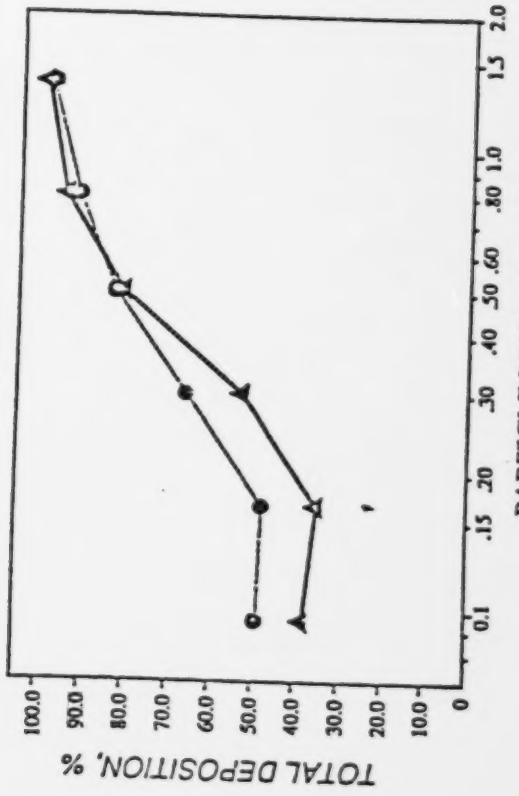
TOTAL DEPOSITION, %
100.0
90.0
80.0
70.0
60.0
50.0
40.0
30.0
20.0
10.0
0
0.1
.15
.20
.30
.40
.50
.60
.80
1.0
1.5
2.0
PARTICLE DIAMETER, μm

FIGURE 8